Editors' Suggestion

All Magic Angles in Twisted Bilayer Graphene are Topological

Zhida Song,[1,*] Zhijun Wang,[2,3,*] Wujun Shi,[4,5] Gang Li,[4] Chen Fang,[2,6,†] and B. Andrei Bernevig[1,7,8,‡]

[1]*Department of Physics, Princeton University, Princeton, New Jersey 08544, USA*
[2]*Beijing National Research Center for Condensed Matter Physics, and Institute of Physics, Chinese Academy of Sciences, Beijing 100190, China*
[3]*University of Chinese Academy of Sciences, Beijing 100049, China*
[4]*School of Physical Science and Technology, ShanghaiTech University, Shanghai 200031, China*
[5]*Max Planck Institute for Chemical Physics of Solids, D-01187 Dresden, Germany*
[6]*CAS Center for Excellence in Topological Quantum Computation, Beijing 100190, China*
[7]*Physics Department, Freie Universitat Berlin, Arnimallee 14, 14195 Berlin, Germany*
[8]*Max Planck Institute of Microstructure Physics, 06120 Halle, Germany*

(Received 28 January 2019; published 16 July 2019; corrected 19 July 2019)

We show that the electronic structure of the low-energy bands in the small angle-twisted bilayer graphene consists of a series of semimetallic and *topological* phases. In particular, we are able to prove, using an approximate low-energy particle-hole symmetry, that the gapped set of bands that exist around *all* magic angles have a nontrivial topology stabilized by a magnetic symmetry, provided band gaps appear at fillings of ± 4 electrons per moiré unit cell. The topological index is given as the winding number (a $\mathbb{Z}$ number) of the Wilson loop in the moiré Brillouin zone. Furthermore, we also claim that, when the gapped bands are allowed to couple with higher-energy bands, the $\mathbb{Z}$ index collapses to a *stable* $\mathbb{Z}_2$ index. The approximate, emergent particle-hole symmetry is essential to the topology of graphene: When strongly broken, nontopological phases can appear. Our Letter underpins topology as the crucial ingredient to the description of low-energy graphene. We provide a four-band short-range tight-binding model whose two lower bands have the same topology, symmetry, and flatness as those of the twisted bilayer graphene and which can be used as an effective low-energy model. We then perform large-scale (11000 atoms per unit cell, 40 days per $\mathbf{k}$-point computing time) *ab initio* calculations of a series of small angles, from 3° to 1°, which show a more complex and somewhat different evolution of the symmetry of the low-energy bands than that of the theoretical moiré model but which confirm the topological nature of the system.

DOI: 10.1103/PhysRevLett.123.036401

Twisted bilayer graphene (TBG) is an engineered material consisting of two layers of graphene, coupled via a van der Waals interaction and rotated relative to each other by some twist angle θ. This material exhibits rich single- and many-body physics [1–4]. Recently, it was suggested that, for $\theta_e \sim 1.1°$, charge gaps appear at fillings of ± 4 electrons per moiré unit cell. Importantly, another charge gap at -2 was also detected and conjectured to be a "Mott gap" [5,6]. If true that the "Mott" state appears, this represents the first many-body phase in zero-field graphene. Upon gating the sample, zero resistivity was observed at low temperatures within a range of carrier density near the Mott gap. The superconductivity in TBG is *conjectured* to be unconventional [7–12]. TBG could be a new platform for the study of strong correlation physics [13–17]. The observed single-particle charge gaps at fillings ± 4 are consistent with the prediction of an earlier theoretical model in Ref. [18], which we call the moiré band model (MBM). In the MBM, the two valleys at K and K' in the graphene Brillouin zone (BZ) decouple. In each valley, the electronic bands of TBG are obtained by coupling the two Dirac cones in the two layers offset in momentum by the angle twist. The model predicts the vanishing of the Fermi velocity at half filling for certain twist angles called the "magic angles," labeled as θ_{mi} with i integers. The predicted first (largest) magic angle is $\theta_{m1} \sim 1.05°$, close to the experimental θ_e, and, therefore, the experimental observation of the narrow bands and "Mott physics" may be related to the vanishing Fermi velocity.

In this Letter, we show, by exhaustive analytical, numerical, and *ab initio* methods, that nontrivial band topology is prevalent in TBG *near every magic angle*, given band gaps appearing at ± 4. We prove that in the MBM for each valley, as long as direct band gaps exist between the middle two bands (not counting spin) and the rest, the two bands possess nontrivial band topology protected by the symmetry C_2T, a composite operation of twofold rotation and time reversal [19–21]. The nontrivial topology is diagnosed both from irreducible representations (irreps) of magnetic groups at high-symmetry momenta as well as from the winding number of Wilson

loops. The proof for arbitrary θ exploits an approximate particle-hole (PH) symmetry in the original MBM; without invoking this symmetry, or if the symmetry is strongly broken, the zero energy bands do not necessarily need to be topological. When the PH symmetry is broken (softly, in the MBM), the statement is proved for $\theta_{m1} \geq \theta \geq \theta_{m6}$ via explicit calculations. We conjecture that the fragile $\mathbb{Z}$ topological index of the two middle bands collapses to a *stable* $\mathbb{Z}_2$ index when more bands are considered.

The nontrivial band topology obstructs the building of a two-band tight-binding model for one valley with correct symmetries and a finite range of hopping. In order to capture the symmetry, dispersion, and topology of the moiré bands, we—for the first time—write down a four-band tight-binding (TB) model defined on the moiré superlattice with short-range hopping. The TB model offers an anchor point for the study of correlation physics in TBG, when interactions are projected to its lower two bands. We test the validity of MBM and of the symmetry eigenvalues used to obtain our TB model by performing large-scale first principles calculations very close to θ_{m1}. Each k point we computed takes about 30–40 days for $\theta \sim \theta_{m1}$. Different from the MBM, we find that the gap at the moiré K point due to the intervalley coupling of graphene changes nonmonotonically as θ decreases. This (along with graphene buckling) could explain the decrease in conductivity at half filling observed in experiments. If this gap is ignored, the density functional theory bands have the same topology with the MBM and TB model.

We now analyze the symmetries of the one-valley MBM. (Please see Sec. II in Ref. [22] for a short review of the MBM.) Because of the vanishing of the K to K' intervalley coupling, any symmetry that relates K to K' in the original layer is hence not present in the one-valley model: Time reversal, C_{6z}, and C_{2y} are absent, but C_{3z}, C_{2x}, and $C_{2z}T$ remain, which generate the magnetic space group (MSG) $P6'2'2$ (No. 177.151 in the BNS notation [40]). Spin-orbit coupling is neglected in the MBM. For the phase at $\theta \gtrsim \theta_{m1}$ in the MBM, where the two bands near the charge neutrality point are disconnected from other bands [A phase in Fig. 1(a)], the irreps of the two bands are calculated to be $\Gamma_1 + \Gamma_2$, $M_1 + M_2$, and $K_2 + K_3$ at the Γ, M, and K points, respectively. (See Table I for the definitions of irreps [41].) Compared to the irreps of elementary band representations (EBRs) [42–44], which represent the atomic limits, listed in Table 1 in Ref. [22], we conclude that these two bands (dubbed 2B-1V for "two-band one-valley") cannot be topologically trivial: They cannot be decomposed into the sum of a positive number of atomic insulators. If we allow coefficients to be negative, we obtain this decomposition: 2B-1V $= s@2c + p_z@1a - s@1a$. Here $s@2c$ represents the band formed by the s orbital at the honeycomb lattice, and $p_z(s)@1a$ represents the band formed by the $p_z(s)$ orbital at the triangular lattice. The negative integer indicates that

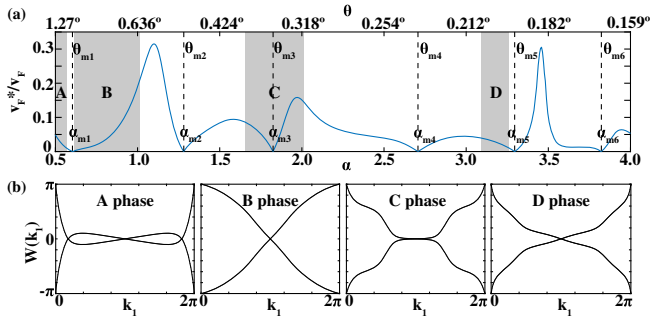

FIG. 1. (a) Fermi velocity at the charge neutrality point of the MBM plotted as a function of the twist angle. The dimensionless parameter $\alpha = w/[2v_F|\mathbf{K}|\sin(\theta/2)]$ uniquely determines the band structure of the MBM (up to a scaling); w is the interlayer coupling, v_F is the Fermi velocity of single-layer graphene, $|\mathbf{K}|$ is the distance between Γ and K, and θ is the twist angle. (See Ref. [18] or Sec. II in Ref. [22] for more details.) In this plot, we set $w = 110$ meV and $v_F|\mathbf{K}| = 19.81$ eV. The gapped regions Θ_a, where the two bands near charge neutrality point are fully disconnected from all other bands, are shadowed with gray and labeled as A–D. The magic angles, where the Fermi velocity vanishes, are marked by dashed lines. By numerical calculation, we find that $\alpha_{m1} \approx 0.605$ ($\theta_{m1} \approx 1.05°$), $\alpha_{m2} \approx 1.28$ ($\theta_{m1} \approx 0.497°$), $\alpha_{m3} \approx 1.83$ ($\theta_{m3} \approx 0.348°$), $\alpha_{m4} \approx 2.71$ ($\theta_{m4} \approx 0.235°$), $\alpha_{m5} \approx 3.30$ ($\theta_{m5} \approx 0.193°$), and $\alpha_{m6} \approx 3.82$ ($\theta_{m6} \approx 0.167°$). (b) The Wilson loops of the four gapped phases have the same winding number, 1.

2B-1V at least hosts a "fragile" topology [42,44,45]; namely, one cannot construct exponentially localized Wannier functions unless they are coupled to some other atomic bands.

As the twist angle decreases away from θ_{m1} in the MBM, the band structure and the irreps at high-symmetry momenta experience nonmonotonic changes, but "magic angles"—where the Fermi velocity at half filling vanishes—reappear periodically. In Fig. 1, we show the evolution of the Fermi velocity as a function of twist angle θ. As a function of θ, the middle two bands are not always separated by a (direct) gap at all momenta: There are four gapped intervals, denoted as Θ_a, where the middle two

TABLE I. Character table of irreps at high-symmetry momenta in magnetic space group $P6'2'2$ (No. 177.151 in BNS settings) [41]. The definitions of high-symmetry momenta are given in Table 1 in Ref. [22]. For the little group of Γ, E, C_3, and C_2' represent the conjugation classes generated from identity, C_{3z}, and C_{2x}, respectively. The number before each conjugate class represents the number of operations in this class. Conjugate class symbols at M and K are defined in similar ways.

	Γ_1	Γ_2	Γ_3		M_1	M_2		K_1	K_2K_3
E	1	1	2	E	1	1	E	1	2
$2C_3$	1	1	−1	C_2'	1	−1	C_3	1	−1
$3C_2'$	1	−1	0				C_3^{-1}	1	−1

bands form a separate group of bands, shaded by gray in Fig. 1. While $\theta_{m3} \in \Theta_a$, $\theta_{m1,m2,m4,m5,m6} \notin \Theta_a$. Therefore, the topology is ill defined for the middle two bands in the MBM at higher magic angles. However, for any $\theta \in \Theta_a$, as well as for smaller angles, we show below that 2B-1V is topologically nontrivial.

Besides the $P6'2'2$ symmetry, the MBM also has an approximate PH symmetry. In the limit of zero rotation of the Pauli matrices of the spin between the two graphene layers, this symmetry is exact—one of the approximations used in Ref. [18]. As we discuss in Sec. II in Ref. [22], this PH symmetry is *unitary* and it *anticommutes* with C_{2x}. The symmetry is crucial in proving a theorem for TBG. We numerically show that our results, understood in the light of the approximate PH symmetry, hold for the general case [46]. First we show that, in the presence of the approximate PH symmetry, for $\theta \in \Theta_a$ 2B-1V has *at least* nontrivial fragile topology. The explicit full proof is given in Secs. II and IV in Ref. [22]. The irreps at K and K' of 2B-1V are always the same as the irreps at K and K' in single-layer graphene. For the irreps of 2B-1V at Γ and M, one uses that the PH symmetry operator anticommutes with C_{2x} but commutes with the other generators of $C_{2z}T$ and C_3. Because of these relations, the upper and the lower irreps have opposite C_{2x} eigenvalues and, hence, form $\Gamma_1 + \Gamma_2$. Similarly, the irreps at M are forced to be $M_1 + M_2$. The bands at any $\theta \in \Theta_a$ have the same irreps at all high-symmetry momenta as those for $\theta \gtrsim \theta_{m1}$ [A phase in Fig. 1(a)]. They then have the same EBR decomposition as the A phase, and we know that the 2B-1V again has fragile topology. The fragile topology can be proved from another perspective. In Sec. IV in Ref. [22], we prove a lemma relating the winding of the Wilson loop eigenvalues of any 2B-1V model to the irreps at high-symmetry momenta, similar to index theorems in Refs. [47–49]. Applying the lemma to the irreps of 2B-1V at any $\theta \in$ any gapped interval, we find the winding to be ± 1 mod 3, i.e., nontrivial.

The irreps cannot, by themselves, distinguish if the winding is even or odd. For the first four gapped phases, we calculate the Wilson loop of 2B-1V and find its winding to always be ± 1. This suggests something stronger: We conjecture that 2B-1V has, in fact, a stable $\mathbb{Z}_2$ topological index protected by $C_{2z}T$. To see this, one realizes that the homotopy group of gapped Hamiltonians in 2D is given by $\pi_2[O(N_{\text{occ}} + N_{\text{unocc}})/O(N_{\text{occ}} \oplus N_{\text{unocc}})] = \mathbb{Z}_2$ for $N_{\text{unocc,occ}} > 2$ and $= \mathbb{Z}$ for $N_{\text{occ}} = 2$, where the latter is nothing but the winding number of Wilson loop eigenvalues. Adding trivial bands to the lowest two bands maps one element in $\mathbb{Z}$ to one $\mathbb{Z}_2$ following the simple rule $z_2 = z \bmod 2$; i.e., odd windings are stable to superposition of trivial bands (see Sec. IV in Ref. [22]). The collapse from $\mathbb{Z}$ classification to $\mathbb{Z}_2$ classification when more bands are considered has been discussed in Ref. [50], and the $\mathbb{Z}_2$ index is identified as the second Stiefel-Whitney class.

Having proved the topological nature of the one-valley model, we note that the two-valley model is just two copies of the one-valley model. As shown in Sec. II in Ref. [22], the irreps of the four bands near charge neutrality are the same as those of two atomic insulators. If we break the valley quantum number by considering the intervalley coupling, a small gap is opened at the K point, and the four bands are now Wannierizable.

We now build short-range hopping models with the correct symmetries and topology, that should be used as toy models for the two topological graphene bands. Because of the topological obstruction, a two-band short-range model with the correct symmetry that simulates 2B-1V is excluded [14,51]. However, we can successfully build a tight-binding four-band, one-valley lattice model with short-range hopping parameters, which has two bands separated by a band gap from another two bands: Either of these two bands is a model for the 2B-1V. We here give the strategy for building this model and leave the details to Sec. V in Ref. [22]. We showed that the irreps ($\Gamma_1 + \Gamma_2$, $M_1 + M_2$, and K_2K_3) of the middle two bands in the one-valley MBM can be written only as a difference of irreps of atomic insulators: $s@2c + p_z@1a - s@1a$. We now reinterpret these irreps differently: From Table 1 in Ref. [22], we see that they can be thought as forming one disconnected branch of the composite bands formed by the sum of s and p_z orbitals sitting on the honeycomb lattice ($2c$). This understanding gives us an ansatz for building the TB model. We start with two independent orbitals (s and p_z) at the honeycomb lattice, which give the irreps $2\Gamma_1$, $2M_1$, and K_2K_3 and $2\Gamma_2$, $2M_2$, and K_2K_3, respectively. We then mix the two EBRs, undergo a phase transition, and decompose the bands into two new branches, each of which has the irreps $\Gamma_1 + \Gamma_2$, $M_1 + M_2$, and K_2K_3—the correct representations of 2B-1V. By this method, the tight-binding model reproduces the irreps of the middle two bands. What is left is to reproduce the correct Wilson loop winding (in principle, it may wind $3n \pm 1$ times). Heuristically, the number of phase transitions gives the winding of the Wilson loop. Since the winding of the Wilson loop is 1 in the 2B-1V model, only one phase transition separates this phase from the phase described by the two orbitals with a gap between them. By this strategy, we obtain the hoppings shown in Fig. 2. Our TB model reproduces both the correct irreps, Wilson loop winding, and flat dispersion.

Our proofs of topology in low-energy TBG are based on the simplified MBM. To give them any credibility, we now must relate our predictions to the realistic calculations of twisted bilayer graphene with negligible spin-orbit coupling. We perform a series of *ab initio* calculations for $i \in \{6, 10, 11\text{–}15, 16, 18, 23, 27, 30\}$, where i denotes the commensurate twist angle by the formula $\theta_i = \arccos(3i^2 + 3i + 0.5/3i^2 + 3i + 1)$ [52]. In our calculations, the distance between the two layers is set to be 3.35 Å. Full band structures are given in Sec. VI in

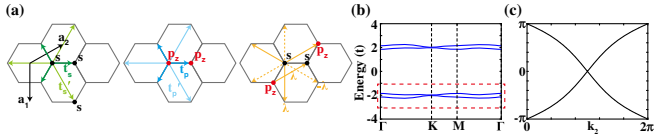

FIG. 2. The four-band tight-binding model for one valley. The *lower* two bands have identical irreps and Wilson loop winding of the gapped middle two bands in the one-valley MBM. (a) The tight-binding model. The energy splitting between s and p_z is Δ. The hopping parameters $t_{s,p}$, $t'_{s,p}$, and λ are all, in general, complex numbers. (b) The band structure. (c) The Wilson loop of the lower two bands. (b) and (c) are calculated with the parameters $t_s = t_p = t$, $t'_s = t'_p = -\frac{1}{3}t$, $\lambda = (2/\sqrt{27})t$, and $\Delta = 0.15t$. As discussed in Sec. V in Ref. [22], such parameters are chosen to flatten the bandwidth.

Ref. [22]. Our *ab initio* calculations show two remarkable features different from the MBM: (i) The PH symmetry breaking is larger, and (ii) the gap at the K point of the moiré BZ is tiny but exists.

In Fig. 3(a), we show the evolution of the *ab initio* energy bands at Γ explicitly. The realistic TBG has two graphene valleys. Thus, the time-reversal symmetry is recovered and the realistic TBG has a higher symmetry group than $P6'2'2$. However, to keep the notations consistent with the one-valley results, we still label the bands by the irreps of $P6'2'2$ (by forgetting the time-reversal symmetry). The gray line stands for the twofold $2\Gamma_2$ band, and the red line stands for the twofold $2\Gamma_1$ band. The two blue lines stand for two different fourfold $2\Gamma_3$ bands. The energies at the Γ point are not PH symmetric: The gap between the lower $2\Gamma_3$ and $2\Gamma_2$ bands is much smaller than that between the higher $2\Gamma_3$ and $2\Gamma_1$ bands. A metallic phase occurs for the middle four bands for $16 < i < 30$, in which the middle four bands are not separated from others. In Fig. 3(b), we calculate the gap at the moiré K point as a function of the twist angles (θ_i). We find the gap at K always exists and varies nonmonotonically as changing

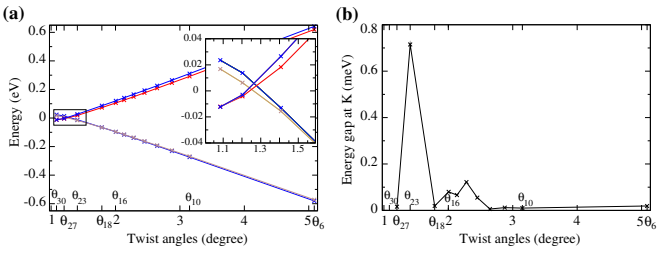

FIG. 3. Electronic band structures with different commensurate twist angles θ_i. (a) The *ab initio* electronic band structures clearly show the breaking of particle-hole symmetry. The bands change nonmonotonically as decreasing θ. The inset is the enlargement of the black box area. The two blue bands indicate two $2\Gamma_3$ bands; the gray band is the $2\Gamma_2$ band; the red band is the $2\Gamma_1$ band. (b) The gap at K at charge neutrality is a function of the twist angle.

theta. In the MBM, no energy difference is expected between two K_2K_3 representations coming from different valleys. However, in *ab initio* calculations of TBG without lattice warping, this is not the case. Because of numerical difficulties, we obtain only the gap for $i = 6, 10, 11$–$15, 16, 18, 23, 27$. We conjecture that the gap at K is not negligible for an extremely small angle. Since the experimental data suggest that the gap is small, we are left with the conclusion that effects not introduced in our *ab initio*, such as lattice relaxation and/or graphene lattice warping, are important and render the gap at the K point much smaller.

In conclusion, we have performed a complete and exhaustive study of the TBG band structure and showed that the low-energy bands are always topological, as long as the lowest two bands are gapped from the rest. We then provided short-range toy tight-binding models for the low-energy TBG, which should (with atomic orbitals matching the charge density of a triangular lattice) be used to study the effects of correlations in graphene. We then checked our results by performing a large set of *ab initio* calculations and presented the areas of agreement and disagreement with the simple, continuum model, as well as possible solutions to these disagreements.

Our work underpins topology as the fundamental property of the low-energy bands of TBG. Here we briefly discuss a few possible effects in the strong correlation physics that may arise from the band topology. When the interaction is smaller than the gap between the 2B-1V and other bands, an efficient way to study the interacting phase is to project the interaction term to the 2B-1V low-energy space. However, since exponentially decaying symmetric Wannier functions are obstructed in the 2B-1V, the symmetric Wannier functions have to be power-law decaying and the projected interaction will become effectively long range, though the original interaction is short range. Novel symmetry-breaking phases and collective modes can appear due to this effective long-range interaction. Another nontrivial effect arising from the band topology is the large superfluid weight in the superconducting phase. In Ref. [53], the authors showed that, when a flat band with nonzero spin Chern number becomes superconducting, the superfluid weight must be larger than a topological lower bound. In Ref. [54], we show that similar effects also happen in TBG: With certain pairing, the superfluid weight in the superconducting phase of the fragile 2B-1V has a lower bound given by the winding number of the Wilson loop.

We thank Barry Bradlyn, Felix von Oppen, Mike Zaletel, Hoi Chun Po for helpful discussions. This work was supported by MOST (No. 2016YFA302400 and No. 2016YFA302600) and NSFC (No. 11674370, No. 11421092, and No. 11504117). Z. S. and B. A. B. were supported by the Department of Energy Grant No. DE-SC0016239, the National Science Foundation

EAGER Grant No. DMR 1643312, Simons Investigator Grants No. 404513, ONR No. N00014-14-1-0330, and NSF-MRSEC No. DMR-142051, the Packard Foundation, the Schmidt Fund for Innovative Research. Z. W. was supported by the National Thousand-Young-Talents Program and the CAS Pioneer Hundred Talents Program. G. L. acknowledges the starting grant of ShanghaiTech University and Program for Professor of Special Appointment (Shanghai Eastern Scholar). The calculations were carried out at the HPC Platform of ShanghaiTech University Library and Information Services, and School of Physical Science and Technology.

Note added.—During the extended period of time that passed while obtaining our *ab initio* results, Ref. [14] has also predicted that the bands at half filling are fragile topological. The differences between our papers are our Letter contains *ab initio* results essential in confirming the nature of the bands and uses the PH symmetry to *prove* all low-energy bands in TBG at *any* angle are topological. Our Letter does not present conjectures or proofs about the Mott phase of TBG. Recently, Ref. [55] proved that the C_2T fragile phase with a nontrivial $\mathbb{Z}_2$ index became Wannierizable after adding atomic bands. This conclusion is not inconsistent with ours, since a stable index does not necessarily imply non-Wannierizability. After a very brief discussion with us, the authors of Ref. [55] posted version 2 of their paper, which identifies a stable index (referred as the second Stiefel-Whitney index). After Ref. [55] appeared, Ref. [56] presented an elaborate study on the Stiefel-Whitney index index and its relation with the Wilson loop.

*Z. S., Z. W. contributed to this work equally.
†cfang@iphy.ac.cn
‡bernevig@princeton.edu

[1] C. R. Dean, A. F. Young, I. Meric, C. Lee, L. Wang, S. Sorgenfrei, K. Watanabe, T. Taniguchi, P. Kim, and K. L. Shepard *et al.*, Nat. Nanotechnol. **5**, 722 (2010).
[2] A. F. Young and L. S. Levitov, Phys. Rev. B **84**, 085441 (2011).
[3] P. Maher, C. R. Dean, A. F. Young, T. Taniguchi, K. Watanabe, K. L. Shepard, J. Hone, and P. Kim, Nat. Phys. **9**, 154 (2013).
[4] B. Hunt, J. Li, A. Zibrov, L. Wang, T. Taniguchi, K. Watanabe, J. Hone, C. Dean, M. Zaletel, R. Ashoori *et al.*, Nat. Commun. **8**, 948 (2017).
[5] Y. Cao, V. Fatemi, A. Demir, S. Fang, S. L. Tomarken, J. Y. Luo, J. D. Sanchez-Yamagishi, K. Watanabe, T. Taniguchi, E. Kaxiras *et al.*, Nature (London) **556**, 80 (2018).
[6] Y. Cao, V. Fatemi, S. Fang, K. Watanabe, T. Taniguchi, E. Kaxiras, and P. Jarillo-Herrero, Nature (London) **556**, 43 (2018).
[7] C. Xu and L. Balents, Phys. Rev. Lett. **121**, 087001 (2018).
[8] B. Roy and V. Juričić, Phys. Rev. B **99**, 121407(R) (2019).
[9] Y.-Z. You and A. Vishwanath, npj Quantum Mater. **4**, 16 (2019).
[10] T. Huang, L. Zhang, and T. Ma, Sci. bull. **64**, 310 (2019).
[11] H. Isobe, N. F. Q. Yuan, and L. Fu, Phys. Rev. X **8**, 041041 (2018).
[12] F. Wu, A. H. MacDonald, and I. Martin, Phys. Rev. Lett. **121**, 257001 (2018).
[13] J. F. Dodaro, S. A. Kivelson, Y. Schattner, X. Q. Sun, and C. Wang, Phys. Rev. B **98**, 075154 (2018).
[14] H. C. Po, L. Zou, A. Vishwanath, and T. Senthil, Phys. Rev. X **8**, 031089 (2018).
[15] B. Padhi, C. Setty, and P. W. Phillips, Nano Lett. **18**, 6175 (2018).
[16] N. F. Q. Yuan and L. Fu, Phys. Rev. B **98**, 045103 (2018).
[17] G. Chen, L. Jiang, S. Wu, B. Lyu, H. Li, B. L. Chittari, K. Watanabe, T. Taniguchi, Z. Shi, J. Jung, Y. Zhang, and F. Wang, Nat. Phys. **15**, 237 (2019).
[18] R. Bistritzer and A. H. MacDonald, Proc. Natl. Acad. Sci. U.S.A. **108**, 12233 (2011).
[19] K. Shiozaki and M. Sato, Phys. Rev. B **90**, 165114 (2014).
[20] C. Fang and L. Fu, Phys. Rev. B **91**, 161105(R) (2015).
[21] C. Fang, Y. Chen, H.-Y. Kee, and L. Fu, Phys. Rev. B **92**, 081201(R) (2015).
[22] See Supplemental Material at http://link.aps.org/supplemental/10.1103/PhysRevLett.123.036401 for detailed information about the TB model and proof of fragile topology, which includes Refs. [23–39].
[23] A. Alexandradinata, Z. Wang, and B. A. Bernevig, Phys. Rev. X **6**, 021008 (2016).
[24] R. Bistritzer and A. H. MacDonald, Phys. Rev. B **81**, 245412 (2010).
[25] C. Bradley and A. Cracknell, *The Mathematical Theory of Symmetry in Solids: Representation Theory for Point Groups and Space Groups* (Oxford University, New York, 2010).
[26] L. Elcoro, B. Bradlyn, Z. Wang, M. G. Vergniory, J. Cano, C. Felser, B. A. Bernevig, D. Orobengoa, G. Flor, and M. I. Aroyo, J. Appl. Crystallogr. **50**, 1457 (2017).
[27] H. C. Po, A. Vishwanath, and H. Watanabe, Nat. Commun. **8**, 50 (2017).
[28] S. Reich, J. Maultzsch, C. Thomsen, and P. Ordejón, Phys. Rev. B **66**, 035412 (2002).
[29] J. Jung and A. H. MacDonald, Phys. Rev. B **87**, 195450 (2013).
[30] S. Fang and E. Kaxiras, Phys. Rev. B **93**, 235153 (2016).
[31] A. H. Castro Neto, F. Guinea, N. M. R. Peres, K. S. Novoselov, and A. K. Geim, Rev. Mod. Phys. **81**, 109 (2009).
[32] B. A. Bernevig, Wannier state of Wannier state (to be published).
[33] W. A. Benalcazar, B. A. Bernevig, and T. L. Hughes, Science **357**, 61 (2017).
[34] A. A. Soluyanov and D. Vanderbilt, Phys. Rev. B **83**, 035108 (2011).
[35] N. Marzari and D. Vanderbilt, Phys. Rev. B **56**, 12847 (1997).
[36] G. Kresse and J. Furthmüller, Phys. Rev. B **54**, 11169 (1996).
[37] G. Kresse and D. Joubert, Phys. Rev. B **59**, 1758 (1999).
[38] P. E. Blöchl, Phys. Rev. B **50**, 17953 (1994).
[39] P. Hohenberg and W. Kohn, Phys. Rev. **136**, B864 (1964).
[40] S. V. Gallego, E. S. Tasci, G. Flor, J. M. Perez-Mato, and M. I. Aroyo, J. Appl. Crystallogr. **45**, 1236 (2012).

[41] B. A. Bernevig *et al.*, Topological Quantum Chemistry for Magnetic Space Group (to be published).
[42] B. Bradlyn, L. Elcoro, J. Cano, M. G. Vergniory, Z. Wang, C. Felser, M. I. Aroyo, and B. A. Bernevig, Nature (London) **547**, 298 (2017).
[43] M. G. Vergniory, L. Elcoro, Z. Wang, J. Cano, C. Felser, M. I. Aroyo, B. A. Bernevig, and B. Bradlyn, Phys. Rev. E **96**, 023310 (2017).
[44] J. Cano, B. Bradlyn, Z. Wang, L. Elcoro, M. G. Vergniory, C. Felser, M. I. Aroyo, and B. A. Bernevig, Phys. Rev. Lett. **120**, 266401 (2018).
[45] H. C. Po, H. Watanabe, and A. Vishwanath, Phys. Rev. Lett. **121**, 126402 (2018).
[46] Four sets of parameters from fitting *ab initio* results at different momenta are used to confirm this statement. Three out of the four angles selected from the four gapped regions are still "gapped" angles for all four different sets; for the fourth angle $\alpha = 3.1$, using set (ii) parameters, 2B-1V is connected to the other bands.
[47] T. L. Hughes, E. Prodan, and B. A. Bernevig, Phys. Rev. B **83**, 245132 (2011).
[48] A. M. Turner, Y. Zhang, and A. Vishwanath, Phys. Rev. B **82**, 241102(R) (2010).
[49] C. Fang, M. J. Gilbert, and B. A. Bernevig, Phys. Rev. B **86**, 115112 (2012).
[50] J. Ahn, D. Kim, Y. Kim, and B.-J. Yang, Phys. Rev. Lett. **121**, 106403 (2018).
[51] J. Kang and O. Vafek, Phys. Rev. X **8**, 031088 (2018).
[52] J. M. B. Lopes dos Santos, N. M. R. Peres, and A. H. Castro Neto, Phys. Rev. Lett. **99**, 256802 (2007).
[53] S. Peotta and P. Törmä, Nat. Commun. **6**, 8944 (2015).
[54] F. Xie, Z. Song, B. Lian, and B. A. Bernevig, arXiv:1805.06906.
[55] H. C. Po, L. Zou, T. Senthil, and A. Vishwanath, Phys. Rev. B **99**, 195455 (2019).
[56] J. Ahn, S. Park, and B.-J. Yang, Phys. Rev. X **9**, 021013 (2019).

Correction: In the front matter, some affiliations were not ascribed properly to the respective authors during the production process; the affiliation attributions have now been corrected.